J Mater Sci: Mater Med (2009) 20:681–689
DOI 10.1007/s10856-008-3613-0

Solid emulsion gel as a novel construct for topical applications: synthesis, morphology and mechanical properties

Kirill I. Shingel · Christophe Roberge · Oleg Zabeida · Marielle Robert · Jolanta E. Klemberg-Sapieha

Received: 11 July 2008 / Accepted: 2 October 2008 / Published online: 24 October 2008

Abstract A series of the solid emulsion gels with the oil volume fraction in the range of 0–50% were synthesized through a polycondensation reaction between activated *p*-nitrophenyl carbonate poly(ethylene glycol) and protein-stabilized oil-in-water emulsions. The resultant structures were investigated in terms of swelling behavior, composition, morphology, mechanical and skin hydration properties. Solid emulsions gels share the properties of both hydrogel and emulsion. Similar to the classical hydrogel, the SEG swells in water up to equilibrium swelling degree, which decreases as the oil volume fraction increases, and comprises immobilized drops of protein-stabilized oil. The impregnation of the oil phase is found to reduce tensile stiffness of the material, but improves material's extensibility. The mechanical properties of the constructs (Young moduli in the range of 9–15 kPa and the elongation at break of 120–220%) are interpreted according to the "rule of elasticity mixture" that considers the elasticity of the composite material to be a sum of the contributions from individual components, i.e. hydrogel and dispersed oil drops. An idealized model that takes into account the history of the material preparation has been proposed to explain the improved extensibility of the constructs. The results of the mechanical tests, equilibrium swelling, and the skin hydration effect of the solid emulsion gels in vivo are discussed from the perspective of the biomedical applications of the solid emulsion gels, in particular, for the transdermal delivery of hydrophilic and lipophilic drugs.

K. I. Shingel (✉) · C. Roberge · M. Robert
Bioartificial Gel Technologies (BAGTECH) Inc.,
400 De Maisonneuve Ouest, Suite 1156, Montreal ,
QC, Canada H3A 1L4
e-mail: kirill.shingel@bagtech.com

O. Zabeida · J. E. Klemberg-Sapieha
Department of Engineering Physics, Ecole Polytechnique,
Box 6079, Station "Centre ville", Montreal,
QC, Canada H3C 3A7

1 Introduction

Recent years have witnessed development of many attractive approaches for overcoming the problems of poor drug solubility and bioavailability of liposoluble compounds, among which oil-in-water nano- and microemulsions are perhaps the most prominent drug delivery solutions [1–3]. The advantages of using oil-in-water emulsions as a drug delivery system are the reduction of drug toxicity, the protection of the active compounds from hydrolysis or oxidation, and the relative ease of the formulation preparation.

As a consequence of the broad exploitation of the emulsion drug encapsulation technology for pharmaceutical use, emulsion-containing hydrogels have recently emerged as a new class of biomaterials [4–7]. These polymer assemblies are designed to integrate dispersed oil drops within an abundant water-rich hydrogel phase and have been shown to present interesting release profiles of lipophilic drugs. Additionally, such emulsion-containing hydrogels may offer the advantage of improved mechanical resistance for easier handling and the opportunity for hydrophilic drug delivery from a hydrogel compartment [5, 7]. Surfactant molecules in these systems are not bound to the matrix and, as noted by some authors, can eventually diffuse from the material along with a drug [5]. This can be considered a drawback of the emulsion-containing hydrogels, since poor biocompatibility, possible toxicity and low clearance rates of the oil-stabilizing components after

penetration can substantially compromise the safety of the emulsion-based drug formulation.

The solid emulsion gels (SEG) described in this work features protein as a natural surfactant that is covalently bound to the matrix and plays a dual role of the network forming component and stabilizer for the apolar phase. This material is synthesized by the bulk polymerization of the protein-stabilized emulsion with bifunctionalized poly(ethylene glycol) molecules. The matrix of the SEG combines all properties of the PEG-protein hydrogel biomaterial, yet it contains oil phase in bioavailable form. Previous study on the in vitro and in vivo bioactivity of the SEG integrated with omega-3 fatty acid revealed the great potential of this drug delivery system [8]; however, structural characterization of the material was incomplete.

Therefore, in this study we synthesized the SEG with varied oil content and performed detailed characterization of the swelling behavior and mechanical properties of the material in order to better understand how the oil volume fraction and the cross-linking influence the overall performance of the polymerized emulsions. The study of the mechanical properties of the SEG was further spurred by the consideration that in contrast to hydrogel structure, where the data on the elasticity, compressibility and tensile strength can directly be used in determining the pore size and solute diffusion characteristics [9], an influence of the inclusion of the apolar phase on the network parameters of the oil-containing structures is hard to anticipate. Also, an ability of the studied material to withstand mechanical stresses is considered a necessary attribute of the construct for the "real life" applications. In view of the above, the data on the composition-dependent physicochemical properties of the SEG seemed very important for tailoring and fine-tuning the material architecture for optimal drug release and bioactivity in vivo.

2 Materials and methods

2.1 Materials

Flaxseed oil was purchased in the nearest health store. Pharmaceutical quality herring oil (omega-3 oil) was from Ascenta Health Ltd (Dartmouth, Nova Scotia, Canada). Pro-Cote® soy polymer (DuPont Soy Polymers, St. Louis, MO, USA) was used as a protein component. Activated poly (ethylene glycol) (PEG) was synthesized in-house by reacting the polymer with nitrophenyl chloroformate [10]. All other reagents purchased from Sigma-Aldrich Chemical Co. (Milwaukee, WI, USA) were of analytical or equivalent grade.

2.2 Synthesis of solid emulsion gels

In the synthesis of solid emulsion gel (SEG), the protein solution (120 mg/ml) was prepared in 0.16 M sodium hydroxide. The protein solution was thoroughly mixed with the oil in the different volume proportions, e.g. 1.0:0.2, 1.0:0.5, 1:1, or 1:2 (protein solution:oil). Different droplet sizes were achieved by varying the intensity of the agitation of the oil–protein mixture. The resultant emulsions were mixed with an aqueous solution of activated PEG (22%, w/v) and the mixture was cast between two films to form a cross-linked emulsion material with a thickness of 1.2 mm. The concentrations of both protein and PEG used in this work have been previously found to be optimal for the hydrogel synthesis [11]. The polymerized SEG was incubated in the buffered solution to wash out *p*-nitrophenol which was formed as a by-product of the polycondensation reaction between PEG *p*-nitrophenyl carbonate ester and soy polymer. The concentration of residual *p*-nitrophenol was lower than 0.5 ppm, as found by HPLC analysis of the SEG extracts [12]. Purified material was formulated with a phosphate buffered saline (PBS) and a preservative at pH 5.5.

2.3 Analysis of the SEG composition

The content of dry residues of PEG-protein conjugates in the SEG was determined gravimetrically after extraction of the oil phase in acetone and drying of the de-fatted material at 60°C until constant weight. Pre-weighed, fully swollen disks of the SEG (~5 cm in diameter) were incubated for 5 h in acetone to leach out the matrix-embedded oil. Acetone was frequently changed to ensure complete extraction. Dry residues of the acetone-washed samples were weighed again to give m_d values. Determination of the water content, m_w, in the oil-containing SEG was carried out by subtracting the weight of the oil-rich dehydrated samples from the initial weight of the fully swollen SEGs, m_s.

The equilibrium water content of the SEG (W_{SEG}) was then determined, using the values of m_w and m_s, as follows:

$$W_{SEG}, \%(\mathrm{w/w}) = 100\frac{m_w}{m_s} \quad (1)$$

Acetone-washed, de-fatted samples of SEG were incubated in aqueous solution in order to saturate the structures with aqueous media. The equilibrium water content (W_{HG}) in the acetone-washed, de-fatted samples of SEG was then determined, using the values of the weights of the swollen network, m_{HG}, and dry residue, m_d.

$$W_{HG}, \%(\mathrm{w/w}) = 100\frac{(m_{HG} - m_d)}{m_{HG}} \quad (2)$$

The density of the material was determined from parallel weighing of the SEG sample in air and water,

using an analytical balance equipped with a specific gravity measurement kit (Shimadzu Corp., Japan). The density of the SEG was then calculated as:

$$\rho_{SEG}\left(\mathrm{g}\cdot\mathrm{cm}^{-3}\right) = \rho_{water}\frac{w_{air}}{w_{air}-w_{water}} \tag{3}$$

where w_{air}, w_{water}, and ρ_{water} are the sample's weight in air, weight in water, and the density of water (0.9973 g cm^{-3} at 24°C), respectively. The values of ρ_{SEG} were used to calculate the volume fraction of the fish oil in the SEG, Φ:

$$\Phi = \frac{m_{oil}}{\rho_{oil}}\frac{\rho_{SEG}}{m_s} \tag{4}$$

where the weight of oil, m_{oil}, is determined as ($m_{oil} = m_s - m_w - m_d$), and the density of fish oil $\rho_{oil} = 0.924$ g cm^{-3} at 24°C.

Swelling behavior of the SEG was also studied in terms of volumetric expansion due to equilibrium swelling after synthesis. Synthesized samples of SEG were cut into round pieces measuring 7 cm in diameter. These samples were immersed in PBS solution to wash out *p*-nitrophenol and to allow the material to swell up to the equilibrium water content. After incubation for 24 h, the diameter of the samples was measured again, and the ratio between final and initial values was considered as the linear expansion factor, f_s.

Assuming three-dimensional isotropic swelling, the theoretical volume fraction of the oil phase in the swollen SEG, Φ_{TH} can be calculated as:

$$\Phi_{TH}(v/v) = \frac{\Phi_{Initial}(v/v)}{f_s^3} \tag{5}$$

The initial volume fraction of the dispersed oil phase, $\Phi_{initial}$ is calculated as an oil-to-PEG and protein solutions volume ratio.

Partial dehydration of the SEG was induced by incubating the material at 45°C. The weight of the samples was permanently monitored during drying. As soon as a necessary dehydration degree seen as a ~10%, 20%, and 50% weight reduction was attained, the samples were rehydrated in the phosphate buffered saline at pH 5.5 and increases in the sample weights due to swelling were recorded.

2.4 Light and environmental scanning electron microscopy

Light microscopy of the SEG was used to calculate the average dimensions of the oil drops. Protein-stabilized emulsion containing 10% oil was mixed with activated PEG solution, and the mixture was immediately cast between two glasses to create a thin film of SEG. Intense vortexing (intense agitation) and gentle shaking (moderate agitation) of the protein–oil mixture was performed in order to control the drop size within the SEG. The agitation time was 5 min in all cases in order to achieve steady drop size distribution [13]. The samples were viewed using a Leica DM4000 B microscope (Leica Microsystems AG, Wetzlar, Germany). The images and the scale (in μm) were recorded, and the particle size distribution was determined in the binary images using the "Analyze particle" option of the ImageJ software (http://rsb.info.nih.gov/ij/). At least three samples of the SEG were analyzed for each conditions of emulsification. The mean volume-surface diameter, D_{32}, was calculated from the drop size distribution, as described elsewhere [13]:

$$D_{32} = \frac{\sum N_i D_i^3}{\sum N_i D_i^2} \tag{6}$$

where N_i is the number of drops of the diameter D_i.

Samples were also observed using an environmental scanning electron microscope (ESEM) Quanta 200 FEG (FEI Company, USA) equipped with a Peltier stage to control the relative humidity by varying temperature and pressure. The pressure was initially set to 4.6 Torr and the temperature was set to 0°C, which according to the phase diagram of water, creates 100% relative humidity. To emphasize the material surface microstructure, the temperature and pressure were then decreased for 10 min to −5°C and 2−3 Torr, respectively, thereby freezing the sample. Subsequently, the temperature was allowed to rise at 2°C/min up to 20°C to sublimate water from the sample at the relative humidity of pure water in the range of 12.5–20% at 2–3 Torr and 20°C inside the chamber.

The pictures obtained from ESEM were re-constructed into 3-D images, using an Interactive 3D Surface Plot plug-in of ImageJ software.

2.5 Evaluation of the mechanical properties

Mechanical properties of the SEG in tensile mode were measured using a slip-peel test instrument (Peel Tester Instrumentors SP-103B-3M45). The measurements were performed under ambient conditions, as described elsewhere [11]. The SEG samples were cut with a punch to ensure a reproducible shape in the dumbbell geometry, according to the D638-03 ASTM standard for the measurement of tensile properties of plastics. The narrow central parts of the samples were 4-cm long and 6-mm wide. The sample thickness was measured using a digimatic micrometer with the resolution of 0.001 mm (Mitutoyo Corp., Japan).

The tensile elastic modulus (E_T) was obtained from the following relation:

$$E_T = \frac{P_T}{\varepsilon_X} \quad (7)$$

where ε_X represents the strains and P_T is the tensile stress that is calculated by dividing the tensile force by the section area of the thinner part of the sample before any deformation [11]. Three specimens were evaluated for each composition of the material.

2.6 Skin hydration study in healthy volunteers

Skin hydration studies were performed on five healthy Caucasian male and female volunteers enrolled in the study after obtaining their written informed consent. The protocol designed in accordance with the principles of ICH for Good Clinical Practice have been reviewed and approved by the Ethic Committee and Regulatory Affairs Department of BioArtificial Gel Technologies Inc. Prior to making measurements, the volunteers stayed under controlled conditions of room temperature (22 ± 0.5°C) and relative humidity (50 ± 5%), for a minimum of 10 min. Test products were applied randomly onto the volar forearms under non-occlusive conditions (two zones on each forearm), and kept in place for 4 h. Determination of the hydration level was performed using a Corneometer® CM825 equipped with a 49 mm^2 probe. Skin hydration levels were evaluated immediately after product removal (t0), and after 30, 60 min, 24, and 72 h post-application. The level of skin hydration measured in the untreated zones of volar forearms was used as the control value. The data were evaluated for statistical significance ($P < 0.05$) by a variance analysis (F-test), followed by the appropriate *t*-test using the Excel statistical package.

3 Results

3.1 Emulsion polymerization

A series of solid emulsion gels were prepared using an increasing content of the dispersed oil phase, while keeping constant the concentration of both PEG and protein in aqueous phase. Prior to polymerization with bi-functionalized PEG, the oil phase is well dispersed in the protein solution, yielding a protein-stabilized emulsion. Such emulsions are stable for several days under ambient condition, but disintegrate completely once the solution of PEG (22%, w/w) is added to the system. However, rapid polymerization of the emulsion after addition of the reactive bi-functionalized PEG cross-linker prevents phase separation and transforms fluid protein-stabilized emulsion into solid emulsion gel in 25–45 s.

Microscopy observations revealed that the applied shear rates affect the size of the protein-stabilized oil droplets. Figure 1a shows the drop size distribution calculated from the light microscopy images of the SEGs made with intense and moderate agitation during oil emulsification. Intense vortexing of the protein–oil mixture results in a relatively narrow drop size distribution centered at the drop diameter of ~7.5 μm, whereas mixing at low shear rates generates high proportion of large drops and broad size distribution (Fig. 1a). The mean volume-surface droplet diameter D_{32} was calculated to be 11.7 and 15.9 μm, for SEGs made from intensively and moderately agitated emulsions, respectively.

Environmental scanning microscopy confirms these observations (Fig. 1b, c). In the micrographs of the SEG made from a well-homogenized emulsion, the droplets of the surface-bound hydrogel-covered oil are visible as numerous vesicles of 5–20 μm in size (Fig. 1b). The size of the drops increases and their number decreases at low shear rates used upon agitation (Fig. 1c). Certain droplets have an irregular shape, indicating that the coalescence of neighboring vesicles might have taken place. Although the hydrogel-covered oil droplets are the predominant morphological feature of the SEG surfaces, hollow cavities are also observed on the surface. In-depth micrographs (Fig. 1d) suggest that the oil vesicles are uniformly dispersed within the volume of the construct.

3.2 Swelling behavior

Despite the presence of the dispersed oil phase, the SEG is able to swell in an aqueous solution until an equilibrium swelling is reached. The swelling degree as well as the expansion factor appears dependent on the initial oil content. Uptake of extra water by SEG inevitably reduces the oil volume fraction. The correlation between the initial and equilibrium oil volume fraction is shown in Fig. 2 along with the theoretical dependence calculated from Eq. 5. The earlier reported values of the expansion factor f and material density ρ_{SEG} (f varies from 1.49 to 1.27 and ρ_{SEG} decreases from 1.013 to 0.987 g × cm^{-3} for the SEG containing 0–50% of the initial oil, respectively) were used for calculations [8]. As can be seen from Fig. 3, the SEG with initial oil content up to 35% (v/v) can be considered as an isotropic swelling material, whereas at higher oil loads, e.g. 50% (v/v), the SEG may comprise a larger oil volume fraction than that expected by assuming an isotropic swelling of the material.

3.3 Component composition

Previous experiments with oil-free hydrogels suggest that the final composition of the swollen material may vary,

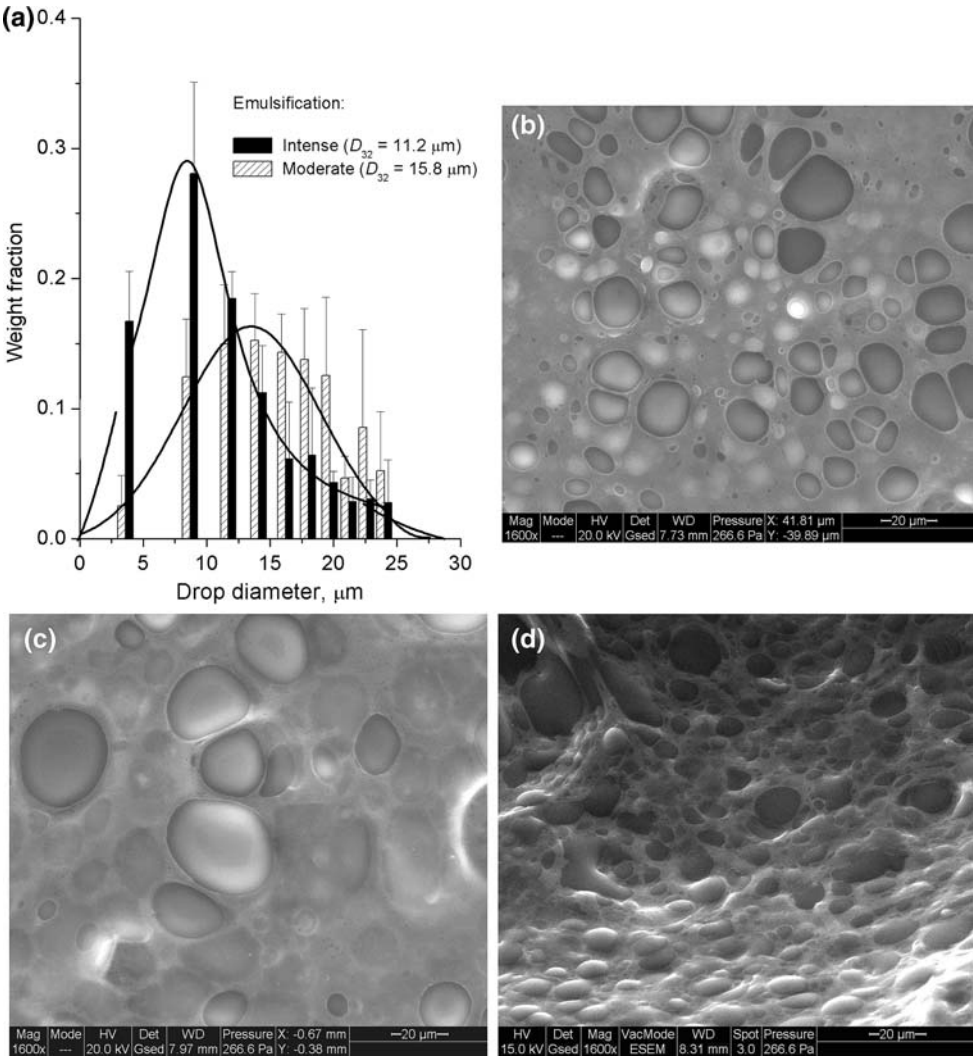

Fig. 1 Drop size distribution (Mean ± SD), as calculated from light microscopy images (**a**) and ESEM appearance of the SEG surface after polymerization of the emulsions prepared upon intense (**b**) and moderate (**c**) agitation ($\Phi \sim 15\%$); **d** In-depth ESEM view of the crashed SEG sample show that the oil drops are distributed uniformly in the material

depending on the type of protein and the efficiency of the PEG–protein polymerization [11, 12]. In this study, in order to verify whether the presence of oil affects the efficiency of the conjugation between PEG and protein, the component composition of the SEG obtained immediately after synthesis was compared with that of fully swollen material (Table 1). The percentage of the polymer retained in the SEG after synthesis and purification increases with increasing oil volume fraction. The total polymer content was additionally normalized to the volume fraction of water in the SEG, since both components of the network, i.e. PEG and soy polymer, are insoluble in the oil phase. The data in the Table 1 shows that the hydrogel component of the SEG is characterized by slightly increased polymer content as the volume of the oil phase increases.

3.4 Mechanical properties

Irrespectively of the oil content in the samples undergoing tensile deformation, stress increases linearly with strain. The variation in the elasticity moduli E_T and the values of maximal elongation as a function of oil volume fraction Φ is shown in Fig. 3. The experimentally observed effect of the oil volume fraction on the material's elasticity modulus was compared with theoretical predictions according to the "rule of elasticity mixture" [14]. The latter considers the elasticity of the composite material to be a sum of the contributions from individual components, i.e.

$$E_T = E_{HG}(1-\Phi) + E_{oil}\Phi = E_{HG} + \Phi(E_{oil} - E_{HG}) \qquad (8)$$

where E_{HG} and E_{oil} are Young's moduli of the hydrogel compartment of the SEG and oil drops, respectively. Young's modulus of oil droplets E_{oil} can be estimated as a triplicate value of the shear modulus, which is given by the Laplace pressure: $2\gamma/R$, where γ is the interfacial tension and R the drop radius [15]. A linear fit of the experimental data in Fig. 3 yields $E_{HG} = 15.2 \pm 0.5$ kPa, which is comparable to the tensile modulus of 17 kPa reported earlier for the oil-free PEG-protein hydrogel [11]. The presence of oil drops reduces overall material stiffness, as

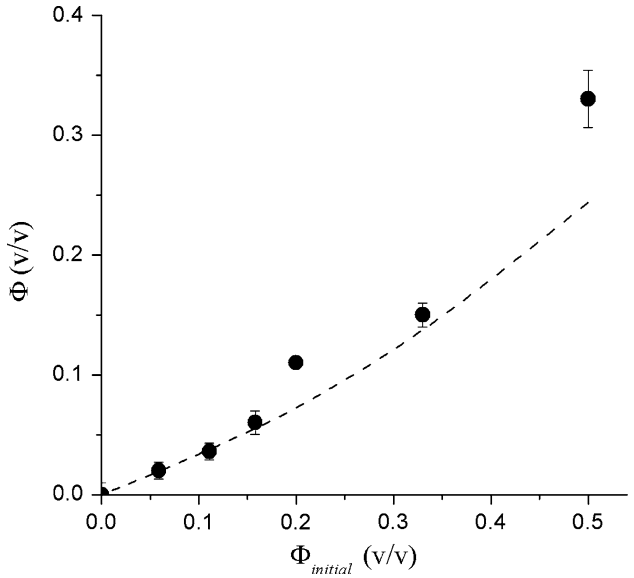

Fig. 2 The correlation between initial ($\Phi_{initial}$) and final (Φ) oil volume fraction in the SEG. Dashed line represents a theoretical dependence between $\Phi_{initial}$ and Φ, as calculated from Eq. 5

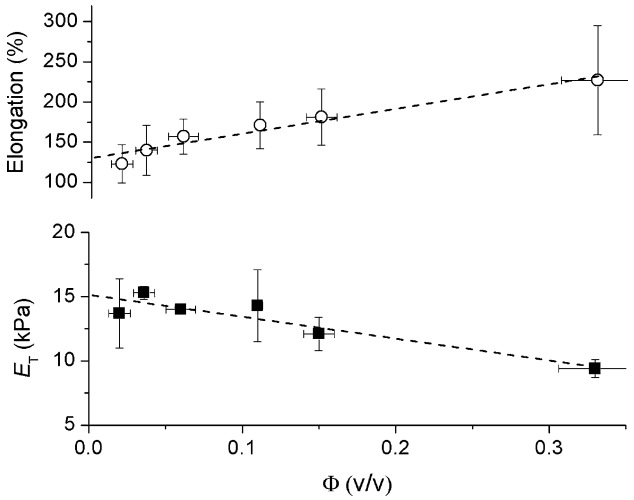

Fig. 3 Variation of the maximal elongation (open circles) and tensile Young's modulus (closed squares) as a function of oil volume fraction. The dashed lines show theoretical dependences calculated using Eq. 8

was judged from the negative slope i.e. $(E_{oil} - E_{HG}) = -17.0 \pm 3.5$ kPa. Notably, the value of $E_{oil} - E_{HG}$ is very close to that of E_{HG}, meaning that the contribution of E_{oil} is negligible. This result supports the approximation that the E_{oil} is zero when oil particles deform more than the matrix [15]. Analysis of the increase of the maximum elongation with increasing oil content (Fig. 3) in terms of elongation additivity shows that the maximal elongation of oil drops is higher than that of the hydrogel domain of the SEG.

Execution of several force application—release cycles at 130% of the sample elongation was detected to provoke permanent deformation of the SEG (data not shown). This pseudo-plastic behavior, a phenomenon that has not been observed for PEG-protein hydrogels, is especially pronounced for oil-rich SEG ($\Phi > 20\%$) and manifests itself after each cycle of force application as an increase in the sample length (by approx. 5%) at a constant stress.

3.5 Skin hydration studies in humans

The level of skin hydration provided by the SEG made with 35% of oil content is compared in Table 2 with that induced by the PEG-protein hydrogel with 95% of equilibrium water content. Application of both products during 4 h provokes a substantial hydration of the skin, which subsides once the materials are removed and returns to basal level after 24 h. No statistically meaningful difference was found in the skin hydration efficiency between water-rich hydrogel and the SEG (Table 2).

3.6 Dehydration and re-swelling

The SEG is noteworthy for retaining its shape and macroscopic integrity after dehydration and re-swelling. The variation of the weights of SEG samples upon gradual drying and subsequent incubation in aqueous solution is shown in Fig. 4. Complete restitution of the original shape and dimensions due to swelling is achieved even in the 50%-dehydrated SEG. It was found, however, that the

Table 1 Polymer and equilibrium water content (Mean (SD)) in the SEG prepared with different initial oil volume fraction and oil-free swollen SEG matrix

Φ	Initial Polymer in SEG, % (w/v)	Polymer in swollen SEG or m_d, % (w/w)	Polymer retained, %	W_{SEG}, % (w/w)[a]	Polymer in aq. phase or m_d/m_w, % (w/w)	W_{HG}, % (w/w)[b]
0	17.0	4.78 (0.01)	28.1	94.91 (0.01)	4.78 (0.01)	94.91 (0.01)
0.06	15.3	4.35 (0.13)	28.4	92.38 (0.01)	4.71 (0.14)	95.17 (0.20)
0.11	13.6	4.38 (0.01)	32.2	85.24 (0.97)	5.34 (0.01)	95.10 (0.07)
0.15	11.3	4.41 (0.02)	38.9	82.04 (0.33)	5.88 (0.03)	94.89 (0.06)
0.33	8.5	3.59 (0.09)	42.2	65.28 (2.38)	5.50 (0.12)	95.94 (0.14)

[a] Calculated from Eq. 1

[b] Calculated from Eq. 2

Table 2 Skin hydration levels (folds from control) following 4 h application of the SEG with 35% of oil and PEG-protein oil-free hydrogel, as measured using Corneometer® (Mean ± SD, $n = 5$)

Time (h)	SEG	Hydrogel
0	1.97 ± 0.51	2.34 ± 0.51
0.5	1.78 ± 0.60	1.42 ± 0.27
1.0	1.40 ± 0.19	1.38 ± 0.20
24.0	1.05 ± 0.16	1.07 ± 0.26
72.0	1.00 ± 0.20	1.05 ± 0.26

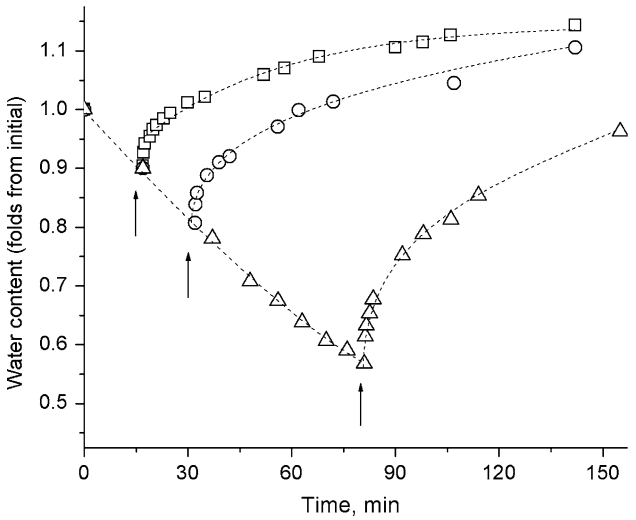

Fig. 4 Reversible swelling of the SEG, as monitored by the changes in the samples weight. The samples were kept at 45°C for gradual drying, followed by incubation of the partially dehydrated material in aqueous solution. The time points when the samples were allowed to swell are shown by arrows

weight of the re-swollen material may exceed its initial value (Fig. 4), indicating that irreversible microscopic changes in the material's structure and integrity have taken place.

Permanent alterations of the SEG's surface topology upon dehydration were registered when ESEM was performed at different values of relative humidity (Fig. 5). As the humidity decreases, the material starts to lose water by evaporation, exposing droplets of the dispersed phase on the surface (Fig. 5a). The loss of water is accompanied by a reduction of the SEG volume, driving individual drops close to each other and promoting their irreversible coalescence (Fig. 5b).

4 Discussion

Solid emulsion gels described in this work share the properties of both hydrogel and emulsion. Similar to the classical hydrogel, the SEG swells in water up to

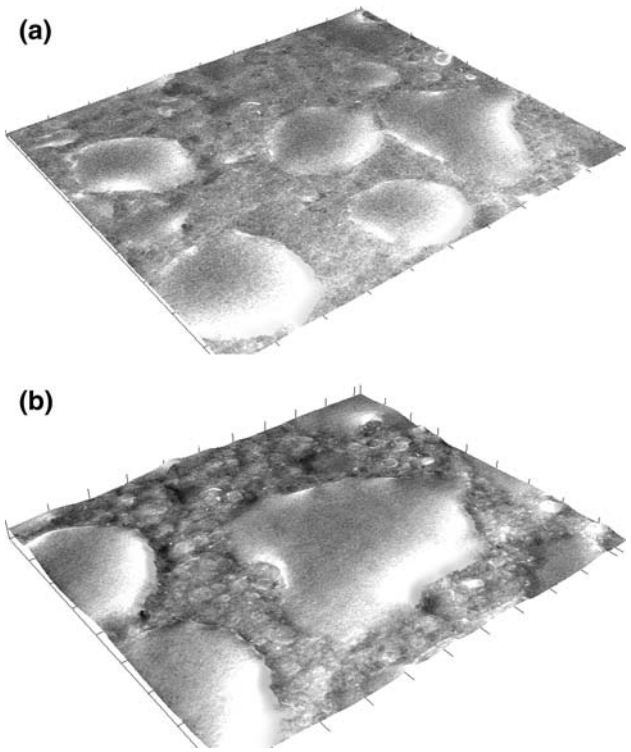

Fig. 5 Coalescence of the neighbouring drops on the surface of the SEG upon dehydration, as observed by ESEM

equilibrium swelling degree and, identical to emulsion, comprises drops of protein-stabilized oil. The shape of the droplets is generally spherical (Fig. 1), as should be expected for a typical emulsion. However, some drops show elliptic shape, indicating that partial drop coalescence takes place during polymerization due to presumable depletion flocculation provoked by PEG chains [16]. Interestingly, emulsion disintegration and phase separation have been reported to be among the most common problems of emulsion polymerization via free radical reactions, thus explaining a limited success of the technique [6]. In our approach for SEG synthesis, the rate of polymerization is by far more important than the rate of phase separation, so despite occasional drops coalescence, the average size of the oil drops after synthesis remains largely unaltered (Fig. 1).

Evaluation of the mechanical properties provides an interesting insight into the structural organization of the SEG. By considering the SEG as a continuous network of a hydrogel with impregnated oil drops we attempted to analyze the influence of the oil phase on Young's modulus of the SEG in terms of van der Poel theory on particle-filled gels [17]. Accordingly, the particles either increase or decrease the material modulus, depending on their inherent stiffness and type of interactions with the matrix [15]. However, this theory appears to be of limited applicability for interpreting mechanical behavior of the SEG. In the

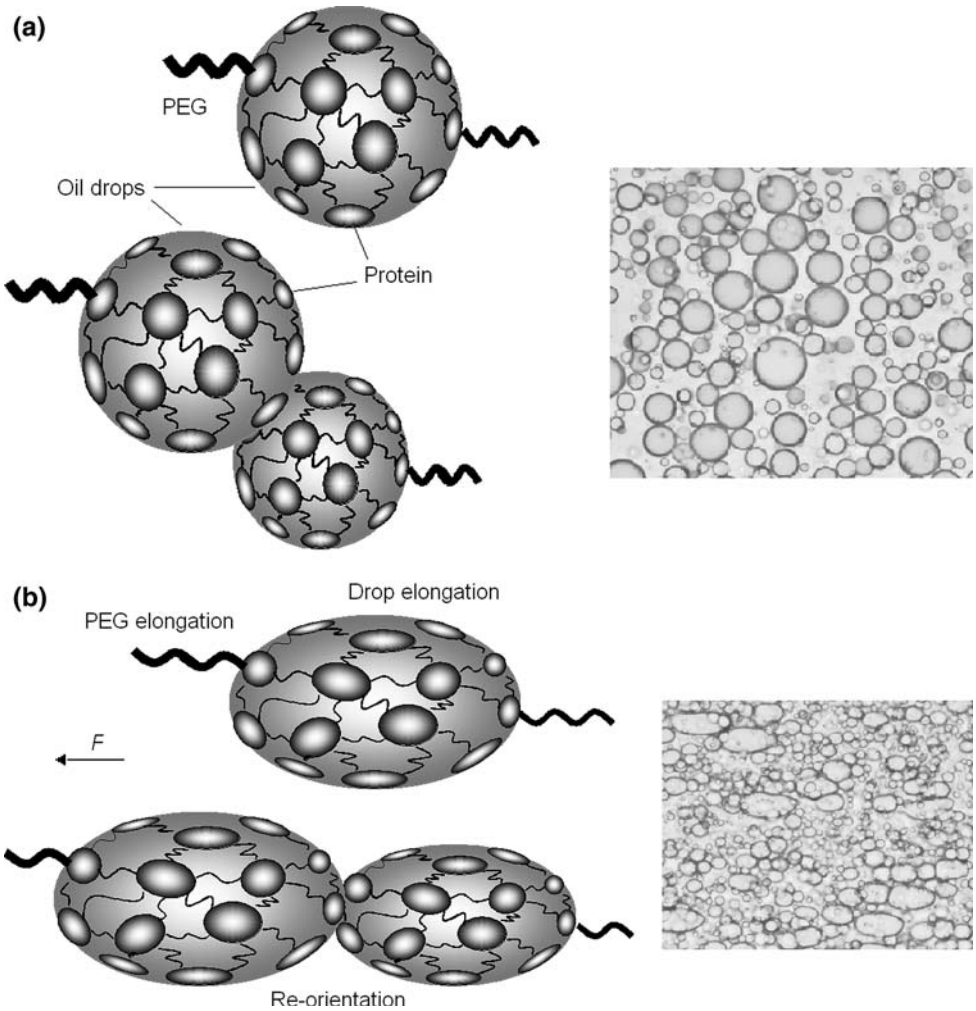

Fig. 6 Idealized model of the response of SEG to the tensile deformation. Drops of oil are immobilized individually and as joined vesicles (**a**). The elongation of the protein-coated oil drops upon deformation contributes to the improved extensibility of the SEG (**b**). Pseudo-plastic deformation is thought to be due permanent re-orientation or "slip" of the joined drops in the direction of the force application

SEG, oil drops reduce Young's modulus of the material and, according to the theory, should behave as an "inactive" filler weakly bound to the matrix [18]. This definition, however, contradicts to the observation that the protein-stabilized drops are cross-linked within the hydrogel domain of the SEG and deforms simultaneously with the material. The oil drops cannot act as "active" filler, since maximal elongation increases with increasing oil content, showing a trend opposite to that expected when filler is tightly bound to the matrix [19]. Therefore, gross mechanical properties of the SEGs with different oil content were described in terms of elasticity additivity (Eq. 8), taking into account the elastic contributions from the hydrogel domain and oil drops (Fig. 3). The results of this analysis indicate that the poor mechanical stiffness of the oil-rich SEG may have originated from a low volume fraction of the elastic hydrogel domain, which itself seems unaffected by the oil and is characterized by a constant Young's modulus ($E_T \sim 17$ kPa). Interestingly, the polymer content in the hydrogel compartment (an indirect indicator of the cross-links density) is largely independent of the oil volume fraction (Table 1), thus affirming validity of our assumption.

An idealized model that takes into account the history of the material preparation has been proposed to explain the improved extensibility of the oil-rich SEG (Fig. 6). Polymerization of the protein moieties at the oil–water interface with activated PEG renders protein-coated drops immobilized individually and in the form of joined vesicles as a result of depletion flocculation by PEG chains (Fig. 6a). Upon deformation the elongation of the protein-coated oil drops precedes or occurs concomitantly with the stretching of the polymer chains (Fig. 6b). A gain in fracture strain due to drop elongation is thus seen as an improved extensibility of the SEG that co-exists with low stiffness of the material. Finally, since drops break-up is unlikely because of high stiffness of the protein layer at the interfaces [20], permanent re-orientation or "slip" of the joined drops in the direction of the force application is hypothesized to be a source of small but noticeable pseudo-plastic deformation (Fig. 6b).

Equilibrium swelling is an original feature of the SEG that distinguishes it from liquid emulsions and emulsion

gels stabilized by comparatively weak physical interactions between components [21, 22]. Although the water content in the SEG structure can be almost two times lower than in a hydrogel, the availability of the aqueous phase and, as a consequence, the skin hydration potential of both structures seems to be comparable (Table 2). Given an inherently good permeability of the skin towards lipids and improved permeability for polar compounds after long-term hydration [23–25], the skin hydration properties of the SEG combined with abundant oil content can be successfully exploited for concomitant transdermal delivery of hydrophilic and hydrophobic compounds. Obvious advantage of this kind of delivery over widely used ointments and creams is that only active lipophilic ingredients penetrate the skin, whereas the oil-stabilizing solid matrix resides outside the body, thereby diminishing the risk of adverse reaction due to penetrated surfactant. Although the possibility of the SEG-mediated delivery of polyunsaturated fatty acids have been recently demonstrated in vivo [8], further studies are now ongoing to confirm the drug delivery potential of the SEG. For example, a dehydration-triggered coalescence of the oil drops on the material surface (Fig. 5) can be beneficially exploited to facilitate deposition of the oil-soluble drugs on the skin surface. The well-known effect of fatty acids in the skin penetration enhancement [26] is also considered to play a role in the transdermal delivery of hydrophobic substances.

In summarizing, in this study we have demonstrated that the rapid polymerization of the protein-stabilized emulsion with reactive bi-functional PEG generates the solid material structures, where dispersed oil phase co-exists with the hydrogel compartment. The material swells up to equilibrium water content and the volume fraction of the oil phase may comprise up to 35% of the construct volume. The impregnation of the oil phase reduces material stiffness, which, however, remains satisfactory for proper handling of the material in topical applications, including drug delivery and wound management. The combination of the dispersed oil phase with hydrogel domain in the SEG along with the possibility of modulating the final composition of the construct can be advantageously exploited for transdermal delivery of both hydrophobic and hydrophilic drugs.

Acknowledgements The authors are thankful to Lucas Poncelet, Maxime Paquette (Department of Engineering Physics, Ecole Polytechnique, Montreal), and Ludmila Anohina and Henadz Isakau (Bioartificial Gel Technologies) for their technical assistance.

References

1. M.J. Lawrence, G.D. Rees, Adv. Drug Deliv. Rev. **45**, 89–121 (2000). doi:10.1016/S0169-409X(00)00103-4
2. M. Kreilgaard, Adv. Drug Deliv. Rev. **54**, S77–S98 (2002). doi:10.1016/S0169-409X(02)00116-3
3. A. Spernath, A. Aserin, Adv. Colloid Interface Sci. **128–130**, 47–64 (2006). doi:10.1016/j.cis.2006.11.016
4. M. Graziacascone, Z. Zhu, F. Borselli, L. Lazzeri, J. Mater. Sci.: Mater. Med. **13**, 29–32 (2002). doi:10.1023/A:1013674200141
5. D. Gulsen, A. Chauhan, Int. J. Pharm. **292**, 95–117 (2005). doi:10.1016/j.ijpharm.2004.11.033
6. C. Holtze, K. Landfester, M. Antonietti, Macromol. Mater. Eng. **290**, 1025–1028 (2005). doi:10.1002/mame.200500241
7. H. Chen, D. Mou, D. Du, X. Chang, D. Zhu, J. Liu, H. Xu, X. Yang, Int. J. Pharm. **341**, 78–84 (2007). doi:10.1016/j.ijpharm.2007.03.052
8. K.I. Shingel, M.P. Faure, L. Azoulay, C. Roberge, R.H. Deckelbaum, J. Tissue Eng. Regen. Med. **3**, 383–393 (2008). doi:10.1002/term.101
9. K.S. Anseth, C.N. Bowman, L.B. Peppas, Biomaterials **17**, 1647–1657 (1996). doi:10.1016/0142-9612(96)87644-7
10. Faure MP, Shingel KI (2008) US Patent No. 7,351,787
11. R. Snyders, K.I. Shingel, O. Zabeida, C. Roberge, M.F. Faure, L. Martinu, J.E. Klemberg-Sapieha, J. Biomed. Mater. Res. **83A**, 88–97 (2007). doi:10.1002/jbm.a.31217
12. K.I. Shingel, M.P. Faure, Biomacromolecules **6**, 1635–1641 (2005). doi:10.1021/bm0492475
13. S. Tcholakova, N.D. Denkov, D. Sidzhakova, I.B. Ivanov, B. Campbell, Langmuir **19**, 5640–5649 (2003). doi:10.1021/la034411f
14. H.S. Kim, S.I. Hong, S.J. Kim, J. Mater. Process. Technol. **112**, 109–113 (2001). doi:10.1016/S0924-0136(01)00565-9
15. T. van Vliet, Colloid Polym. Sci. **266**, 518–524 (1988). doi:10.1007/BF01420762
16. N.K. Pandit, J. Kanjia, K. Patel, D.G. Pontikes, Int. J. Pharm. **122**, 27–33 (1995). doi:10.1016/0378-5173(95)00032-E
17. C. van der Poel, Rheol. Acta **1**, 198–205 (1958). doi:10.1007/BF01968867
18. C.M. Wijmans, E. Dickinson, J. Chem. Soc. Faraday Trans. **94**, 129–137 (1998). doi:10.1039/a706632e
19. G. Sala, G.A. van Aken, M. Cohen Stuart, F. van de Velde, J. Texture Stud. **38**, 511–535 (2007). doi:10.1111/j.1745-4603.2007.00110.x
20. F.E. Mitidieri, J.R. Wagner, Food Res. Int. **35**, 547–557 (2002). doi:10.1016/S0963-9969(01)00155-7
21. C. Solans, J.G. Dominguez, J.L. Parra, J. Heuser, S.E. Friberg, Colloid Polym. Sci. **266**, 570–574 (1988). doi:10.1007/BF01420770
22. N. Drelon, F. Leal-Calderon, Langmuir **23**, 4792–4799 (2007). doi:10.1021/la070071c
23. R.O. Potts, M.L. Francoeur, J. Invest. Dermatol. **96**, 495–499 (1991). doi:10.1111/1523-1747.ep12470197
24. V.H. Mak, R.O. Potts, R.H. Guy, Pharm. Res. **8**, 1064–1065 (1991). doi:10.1023/A:1015873511692
25. H. Tang, D. Blankschtein, R. Langer, J. Pharm. Sci. **91**, 1891–1907 (2002). doi:10.1002/jps.10177
26. T.M. Suhonen, J.A. Bouwstra, A. Urtti, J. Control Release **59**, 149–161 (1999). doi:10.1016/S0168-3659(98)00187-4